C. R. Chimie 18 (2015) 1277–1283

Contents lists available at ScienceDirect

Comptes Rendus Chimie

www.sciencedirect.com

Full paper/Mémoire

Generation of a substituted 1,2,4-thiadiazole ring via the [3+2] cycloaddition reaction of benzonitrile sulfide toward trichloroacetonitrile. A DFT study of the regioselectivity and of the molecular mechanism

Saeedreza Emamian

Chemistry Department, Shahrood Branch, Islamic Azad University, Shahrood, Iran

ARTICLE INFO

Article history:
Received 20 July 2015
Accepted after revision 10 September 2015
Available online 3 November 2015

Keywords:
Thiadiazoles
Benzonitrile sulfides
[3+2] cycloaddition reactions
Regioselectivity
ELF topological analysis
Parr functions

ABSTRACT

A theoretical study of the [3+2] cycloaddition (32CA) reaction between benzonitrile sulfide **BNS1** and trichloroacetonitrile **TCAN2** at the MPWB1 K/6-311G(d) level was undertaken. Among two feasible C1–N5 and C1–C4 regioisomeric channels, the former is completely preferred, in the presence of toluene, over the latter, both kinetically, $\Delta\Delta G_{activation}$ = 17.5 kcal/mol, and thermodynamically, $\Delta\Delta G_{reaction}$ = −12.8 kcal/mol, in excellent agreement with experimental outcomes. The strong global electrophilic and nucleophilic characters found for **TCAN2** and **BNS1**, respectively, allow the studied 32CA reaction to take place via a polar process. Interestingly, the analysis of the TSs geometries clarifies that in the case under study, regioselectivity is controlled by destabilizing steric repulsion interactions rather than electronic ones. The ELF topological patterns indicate that while the formation of S3–C4 single bond takes place exactly according to Domingo's model, that of the C1–N5 single bond is a direct consequence of the nucleophilic attack of the C5 carbon atom on the N5 nitrogen atom supporting a *two-stage one-step* molecular mechanism.

1. Introduction

A rapid construction of five-membered heterocyclic compounds in a highly regio- and stereoselective manner can be realized via [3+2] cycloaddition (32CA) reactions as a valuable synthetic utility [1–3]. A 32CA reaction makes sense when a three-atom-component (TAC) is attacked with an unsaturated bond to produce the corresponding five-membered cycloadduct. The aforementioned reactions are well known among most chemists as "1,3-dipolar" cycloadditions in which a "1,3-dipole" species reacts with a "dipolarophile". Nevertheless, using "TAC" for "1,3-dipole" and "[3+2]" instead of "1,3-dipolar" provides a more realistic portrait of the nature of the species involved and the mechanistic facts of these reactions [4].

The electronic nature of the TACs involved in 32CA reactions allows these reactions to be classified as *pseudodiradical-type* (*pr-type*) reactions including TACs with a high pseudodiradical character, such as carbonyl ylides, and *zwitterionic-type* (*zw-type*) reactions comprising TACs with a high zwitterionic character, e.g., nitrile oxides. While *pr-type* 32CA reactions take place easily via an early transition state (TS) with non-polar character, favorable electrophilic/nucleophilic interactions proceed via *zw-type* 32CA reactions through polar TSs [5,6]. Similarly, TACs are classified into two different categories: allylic-type TACs (A-TACs), presenting a bent geometrical structure, and the propargylic type TACs (P-TACs)

E-mail addresses: s_emamian@iau-shahrood.ac.ir, saeedreza_em@yahoo.com.

http://dx.doi.org/10.1016/j.crci.2015.09.003
1631-0748/

displaying a linear geometrical structure including a triple bond. As depicted in Scheme 1, the electronic structure of A- and P-TACs can generally be represented using five resonant Lewis structures [6].

Among the represented structures, while Lewis structures I through IV have closed-shell zwitterionic electronic structures, Lewis structure V has an open-shell singlet-diradical electronic structure. On the other hand, Lewis structures III and IV, with a negligible contribution among structures I through V, are the only 1,3-dipoles [6] clarifying why the "1,3-dipole" phrase should not be predicated to these compounds when participating in 32CA reactions. Indeed, it has been well established that Lewis structure V plays a key role in the reactivity of both A- and P-TACs in 32CA reactions [4,7].

The 32CA reaction of nitrilium betaines ($RC{\equiv}N^{+}{-}X^{-}$, X = CR_2, NR, O, and S), a well-known class of P-TACs, toward activated double or triple bonds is extensively employed in order to synthesize five-membered heterocycles including C=N–X framework [8]. Even though the 32CA reaction of nitrile ylides, X = CR_2, nitrile imines, X = NR, and nitrile oxides, X = O, have widely been explored [9–16], the only other nitrilium betaine, namely nitrile sulfides, X = S, have received much less attention in 32CA reactions [17]. The first appearance of nitrile sulfides was evidenced by Franz and Black [18]. While some nitrile oxides are allowed to be isolated and characterized at room temperature, all nitrile sulfides are thermally unstable and easily participate in the decomposition processes. Consequently, their generation in situ should essentially be observed for productive purposes of this kind of nitrilium betaines. In this regard, the most widely used procedure is the thermal decomposition of five-membered heterocycles that already contain a C=N–S framework, e.g., 1,3,4-oxathiazo1-2-ones (Scheme 2) [19].

The high reactivity of nitrile sulfides in 32CA reactions toward electrophilically activated alkenes [20], alkynes [21], nitriles [22], as well as carbonyl [23] and thiocarbonyl [24] compounds, has been documented.

Thiadiazoles, the aromatic five-membered heterocycles comprising C, N, and S atoms, can simply be prepared through in situ generation of nitrile sulfides in the presence of activated nitriles [25,26]. Thiadiazoles derivatives have a comprehensive spectrum of pharmacological and biological activities such as anticancer, anticonvulsant, anti-inflammatory, carbonic anhydrase inhibitory, analgesic, antioxidant, antidiabetic, antibacterial, antifungal and antitubercular properties [27–32]. The 32CA reaction of benzonitrile sulfide, **BNS1**, toward trichloroacetonitrile,

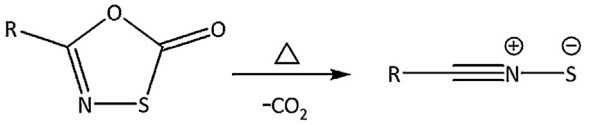

Scheme 2. Thermal decomposition of 1,3,4-oxathiazo1-2-ones yielding nitrile sulfides.

TCAN2, has experimentally been studied by Greig et al., 1986 [33]. Regardless of the long time passed since this experimental consideration, a theoretical study is capable of clarifying some noticeable and challengeable points, particularly from a mechanistic point of view, about the investigated 32CA reaction in which C–N and C–S interactions play a main role in bonding development along the reaction coordinate.

Herein, a density functional theory (DFT) study of the 32CA reaction between **BNS1** and **TCAN2**, as presented in Scheme 3, is performed at the MPWB1 K/6-311G(d) level in order to characterize the energetic, complete regioselectivity, and the reaction mechanism of this process. Moreover, an electron localization function (ELF) [34–37] topological analysis of the most relevant points along the intrinsic reaction coordinate (IRC) [38] curve of the 32CA reaction between **BNS1** and **TCAN2** is carried out. Such ELF analysis characterizes the bonding changes along the studied 32CA reaction and nicely portrays the patterns associated with the breaking of C1–N2 and C4–N5 bonds in reagents, and the formation of C1–N5 and C4–S3 bonds between reagents, establishing the molecular mechanism of this reaction in detail.

2. Computational details

The recent valuable results provided by Truhlar's research group indicate that the MPWB1 K hybrid meta density functional method (HMDFT) gives good results for thermochemistry and thermochemical kinetics as well as excellent saddle-point geometries [39]. Consequently, in the present study, DFT computations were carried out using the MPWB1 K exchange-correlation functional, together with the standard 6-311G(d) basis set [40]. The Berny analytical gradient optimization method using GEDIIS [41] was employed in geometry optimization steps. The stationary points were characterized by frequency calculations in order to verify that TSs have one and only one imaginary frequency. The IRC paths [38] were traced in order to check the energy profiles connecting each TS with the two associated minima of

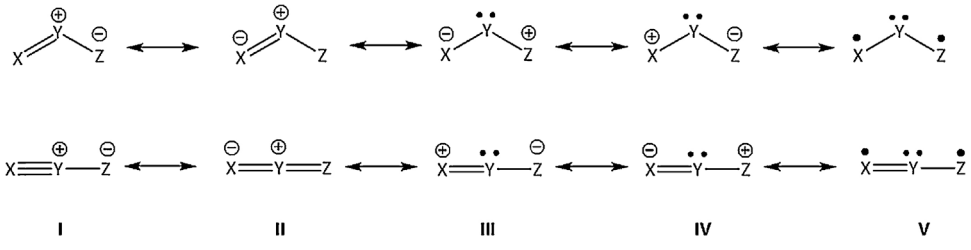

Scheme 1. Schematic representation of five resonant Lewis structures for an A-TAC (top) and a P-TAC (bottom).

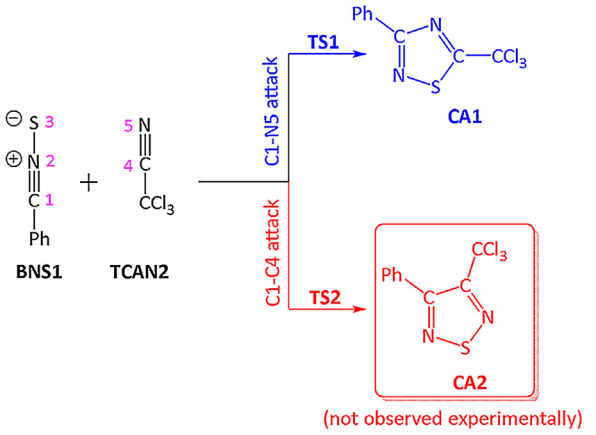

Scheme 3. (Color online.) Reaction paths involved in the 32CA reaction between benzonitrile sulfide **BNS1** and trichloroacetonitrile **TCAN2**.

the proposed mechanism using the Hessian-based Predictor–Corrector (HPC) integrator algorithm [42]. Solvent effects of toluene ($\varepsilon = 2.37$) were taken into account in the optimizations using the polarizable continuum model (PCM), as developed by Tomasi's group [43] in the framework of the self-consistent reaction field (SCRF) [44]. Enthalpy, entropy, and Gibbs free energy values in the gas phase as well as in the presence of toluene were calculated with standard statistical thermodynamics at 298 K and 1 atm [40]. The electronic structures of the stationary points were analyzed by the natural bond orbital (NBO) method [45]. The ELF study was performed with the TopMod program [46] using the corresponding monodeterminantal wave functions of the selected structures along the IRC curve. All computations were carried out with the Gaussian 09 suite of programs [47].

The global electrophilicity index ω [48] is given by the following expression, $\omega = \mu^2/2\eta$ based on the electronic chemical potential, μ, and on the chemical hardness, η. Both quantities may be approached in terms of the one-electron energies of the frontier molecular orbitals HOMO and LUMO, ε_H and ε_L, as $\mu \approx (\varepsilon_H + \varepsilon_L)/2$ and $\eta \approx (\varepsilon_L - \varepsilon_H)$, respectively [49]. The global nucleophilicity index N [50], based on the HOMO energies obtained within the Kohn–Sham scheme [51], is defined as $N = \varepsilon_{HOMO}$ (Nu) $- \varepsilon_{HOMO}$ (TCE), in which (Nu) denotes the given nucleophile. This relative nucleophilicity index refers to tetracyanoethylene (TCE). P_k^- and electrophilic P_k^+ Parr functions [52] were obtained through the analysis of the Mulliken atomic spin density (ASD) of the radical cation of **BNS1** and of the radical anion of **TCAN2**, respectively.

3. Results and discussion

The present study is divided into three parts:

- first, as depicted in Scheme 3, the reaction paths involved in the 32CA reaction of **BNS1** with **TCAN2** yielding the corresponding cycloadducts **CA1** and **CA2** (thiadiazole regioisomers) are studied;
- in the second part, an analysis of the global and local DFT reactivity indices of the reagents involved in the considered 32CA reaction is performed in order to explain the reactivity and the complete regioselectivity displayed by the cycloaddition between **BNS1** and **TCAN2**;
- in the third part, an ELF topological analysis along the 32CA reaction of **BNS1** toward **TCAN2** is carried out in order to characterize the molecular mechanism in this cycloaddition.

3.1. Study of the reaction paths involved in the 32CA reaction of BNS1 toward TCAN2

Due to the asymmetry of both reagents, two competitive channels are feasible for the 32CA reaction between **BNS1** and **TCAN2**. They are related to the two regioisomeric approach modes of the C1 carbon atom of **BNS1** toward the N5 (via C1–N5 attack) or C4 (via C1–C4 attack) atoms of **TCAN2** (see Scheme 3 for atom numbering). An analysis of the stationary points involved in the two regioisomeric paths indicates that this 32CA reaction takes place through a one-step mechanism. Consequently, two TSs, **TS1** and **TS2**, and two corresponding formal [3+2] cycloadducts, **CA1** and **CA2**, were located and characterized on the potential energy surface (PES) of this reaction. Relative enthalpies, ΔH, entropies, ΔS, and Gibbs free energies, ΔG, for the species involved in the 32CA reaction between **BNS1** and **TCAN2** in the gas phase as well as in the presence of toluene are displayed in Table 1. As displayed in Table 1, activation enthalpies associated with the regioisomeric **TS1** and **TS2** in the gas phase are 7.8 and 23.3 kcal/mol, respectively. These values clearly indicate that the C1–N5 regioisomeric pathway (Scheme 3) is the unique channel that can kinetically be reached. On the other hand, the gas-phase reaction enthalpies corresponding to the regioisomeric cycloadducts are –59.3 (**CA1**) and –47.2 (**CA2**) kcal/mol, demonstrating the high exothermic nature of the 32CA reaction, studied particularly in the reachable C1–N5 channel. It is worth noting that the strong exothermicity of the studied 32CA reaction is a direct consequence of the resonance stabilizing energy released during the formation of the corresponding aromatic cycloadducts. Due to the bimolecular nature of the 32CA reactions, as shown in the third column of Table 1, both activation and reaction entropies become very negative, acting as unfavorable factors in the formation of TSs and CAs. When the unfavorable activation term, $T\Delta S$, is added to the enthalpy changes, a significant increase is produced in the activation and reaction Gibbs free energies (see the fourth column of Table 1). Because of the noticeable contribution of the $T\Delta S$ term, the gas phase activation and reaction Gibbs free energies associated with the more favorable C1–N5 channel become 20.6 (**TS1**) and –44.2 (**CA1**) kcal/mol, displaying a noteworthy rise compared with the corresponding enthalpy values. Relative Gibbs free energies perceptibly imply that the 32CA reaction between **BNS1** and **TCAN2** in the gas phase takes place via a strongly regioselective (regiospecific) fashion, passing through **TS1** ($\Delta\Delta G_{activation} = 17.4$ kcal/mol) yielding **CA1**

Table 1
MPWB1 K/6-311G(d) relative[a] enthalpies, ΔH, entropies, ΔS, and Gibbs free energies, ΔG, of the species involved in the studied 32CA reaction.

Species	Gas			Toluene		
	ΔH (kcal/mol)	ΔS (cal/mol·K)	ΔG (kcal/mol)	ΔH (kcal/mol)	ΔS (cal/mol·K)	ΔG (kcal/mol)
BNS1						
TCAN2						
TS1	7.8	−42.9	20.6	9.9	−41.6	22.4
TS2	23.3	−49.1	38.0	25.2	−49.0	39.9
CA1	−59.3	−50.5	−44.2	−56.7	−50.3	−41.7
CA2	−47.2	−54.0	−31.0	−44.8	−53.5	−28.9

BNS1: benzonitrile sulfide; **TCAN2**: trichloroacetonitrile.
[a] Relative to separate **BNS1** and **TCAN2**.

($\Delta\Delta G_{reaction}$ = −13.2 kcal/mol) as the unique kinetically and thermodynamically reachable cycloadduct.

When solvent effects of toluene are taken into account, due to larger solvation of the reagents than of TSs and of cycloadducts, not only the activation Gibbs free energies increase, but also the exergonic nature of reaction is reduced (see the last column of Table 1). The relative Gibbs free energy profile associated with the 32CA reaction of **NBS1** toward **TCAN2** in the presence of toluene is presented in Fig. 1. This profile, in complete agreement with experimental findings [33], obviously demonstrates that the studied 32CA reaction in the presence of toluene, although under some harsher conditions with respect to the gas phase, takes place through the regiospecific C1–N5 channel affording **CA1** as the unique observable formal [3+2] cycloadduct. In other words, while the total regioselectivity in the gas phase remains unchanged in the presence of solvent, neither kinetics nor thermodynamics of 32CA reaction between **BNS1** and **TCAN2** can be affected by the inclusion of solvent effects; a characteristic which is expected for 32CA reactions.

The optimized structures of TSs involved in the studied 32CA reaction in toluene including some selected bond lengths together with the unique imaginary frequencies are given in Fig. 2.

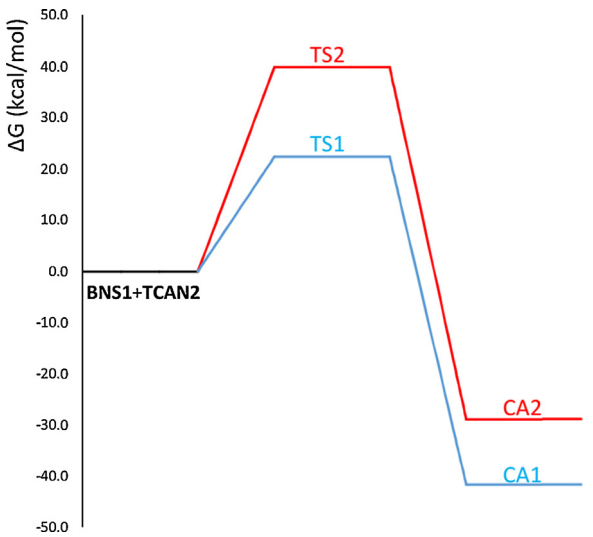

Fig. 1. MPWB1 K/6-311G(d) relative Gibbs free energy profile of the 32CA reaction of **BNS1** toward **TCAN2** in the presence of toluene.

The electronic nature of the 32CA reaction between **BNS1** and **TCAN2** was analyzed by computing the global electron density transfer (GEDT) [53] at the corresponding TSs. In order to calculate the GEDT, the natural atomic charges at the TSs of the two regioisomeric channels, obtained through a natural population analysis (NPA), were shared between the nitrone and the thioketone frameworks. In gas phase, the GEDT that fluxes from the benzonitrile sulfide moiety toward the trichloroacetonitrile one is 0.27e at **TS1** and 0.25e at **TS2,** implying a relatively high polar nature for the investigated 32CA reaction.

3.2. DFT analysis based on the global and local reactivity indexes

Global reactivity indices defined within the conceptual DFT [54] are powerful tools to explain the reactivity and regioselectivity in the cycloaddition reactions. The global indexes, namely, electronic chemical potential (μ), chemical hardness (η), global electrophilicity (ω), and global nucleophilicity (N) for **BNS1** and **TCAN2** are presented in Table 2. As presented in this table, the electronic chemical potential of **BNS1**, −4.00 eV, is higher than that of **TCAN2**, – 5.59 eV, allowing the GEDT to take place along the corresponding polar 32CA reaction from **BNS1** toward **TCAN2**, in quite good agreement with the GEDT analysis performed on the corresponding TSs (see earlier).

BNS1 has a low global electrophilicity ω index, 1.46 eV, and a high nucleophilicity N index, 3.65 eV, being classified as a marginal electrophile and a strong nucleophile within the electrophilicity [55] and nucleophilicity [56] scales. On the other hand, while **TCAN2** has a high global electrophilicity ω index, 1.59 eV, classified as a strong electrophile, corresponding to a negative global nucleophilicity index, –0.10 eV, reveals that this species does not present any nucleophilic character. It should be noted that, as mentioned in section 2, in the definition of the global nucleophilicity index, TCE is taken into account as a reference; *i.e.* the species with the most non-nucleophilic character (N = 0.00 eV). The analysis of these global indices indicates that along a polar 32CA reaction, **BNS1** and **TCAN2** will act as nucleophile and electrophile, respectively.

When an electrophile–nucleophile pair is approached, the most favorable reactive channel is that associated with

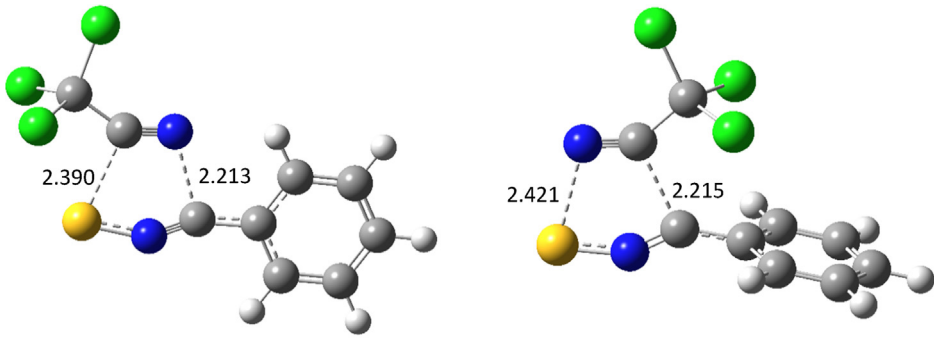

Fig. 2. MPWB1 K/6-311G(d) optimized geometries of TSs involved in the 32CA reaction between **BNS1** and **TCAN2** in the presence of toluene, including some selected bond distances, in Å, and the corresponding unique imaginary frequencies, in cm^{-1}.

the initial two-center interaction between the most electrophilic center of the electrophile and the most nucleophilic center of the nucleophile. Recently, Domingo has proposed the nucleophilic P_k^- and electrophilic P_k^+ Parr functions [52], derived from the excess of spin electron density reached via the GEDT process from the nucleophile to the electrophile as a powerful tool in the study of the local reactivity in polar processes. Since **BNS1** and **TCAN2** act as nucleophile and electrophile, respectively, in the studied 32CA reaction, the nucleophilic P_k^- Parr functions of **BNS1** and the electrophilic P_k^+ Parr functions of **TCAN2** are calculated and depicted in Fig. 3. As shown in this figure, while the S3 sulfur atom in **BNS1** is the most nucleophilic center possessing the maximum nucleophilic Parr function value of 0.89, the most electrophilic center in **TCAN2** is the N5 nitrogen atom possessing the maximum electrophilic Parr function value of 0.26 (atom numbering is given in Scheme 3). Therefore, it is predicted that the most favorable electrophile–nucleophile interaction along the electrophilic attack of **TCAN2** on **BNS1** should be that between the most electrophilic center of **TCAN2**, the N5 nitrogen atom, and the most nucleophilic center of **BNS1**, the S3 sulfur atom. This prediction is in complete disagreement with the energetic studies provided in Section 3.1. Therefore, it seems that steric repulsion interactions play a more important role than electronic effects in the regioselectivity of the studied 32CA reaction. A closer attention to Fig. 2 evidences that the steric repulsion interaction between the large chlorine substitutions and phenyl ring, on the one hand, and the steric hindrance between the lone pairs of S3 sulfur and N5 nitrogen atoms, on the other hand, account for the lack of predominance of TS2 over TS1. Interestingly, not only the aforementioned steric repulsions are absent from TS1 but also a stabilizing weak hydrogen bonding interaction between the lone pair of N5 nitrogen atom and the neighboring hydrogen atom of phenyl ring leads to a significant difference in relative Gibbs free energies of **TS1** and **TS2** (Table 1).

Table 2
MPWB1 K/6-311G(d) global electronic chemical potential, μ, global hardness, η, global electrophilicity, ω, and global nucleophilicity, N, in eV, for **BNS1** and **TCAN2**.

	μ	η	ω	N
BNS1	−4.00	5.49	1.46	3.65
TCAN2	−5.59	9.82	1.59	−0.10

BNS1: benzonitrile sulfide; **TCAN2**: trichloroacetonitrile.

3.3. ELF topological analysis of the 32CA reaction between BNS1 and TCAN2

The electron density, $\rho(r)$, of a molecular system can represent all information hidden in the wave function of such a system. Thus, a successive detection of the electron density changes along a chemical reaction in which a continuous redistribution of $\rho(r)$ proceeds in the course of the reaction can provide valuable information about bonds forming/breaking patterns. In this way, from the molecular mechanistic point of view, our questions can greatly be addressed [57]. One of the most popular functions, introduced by Becke and Edgecombe [58], is the electron localization function, ELF, from which essential information

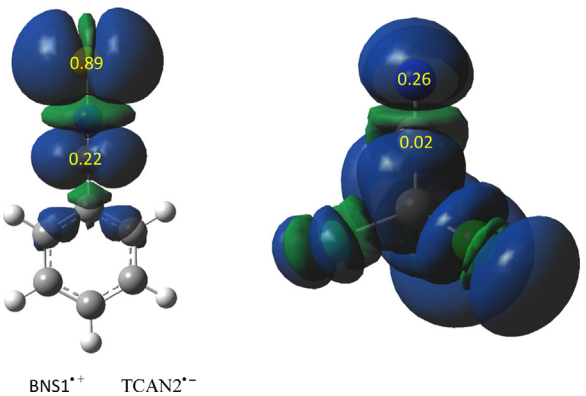

Fig. 3. MPWB1 K/6-311G(d) maps of the Mulliken atomic spin density (ASD) of the radical cation $BNS1^{\bullet+}$ and the nucleophilic P_k^- Parr function of **BNS1**, and ASD of the radical anion $TCAN2^{\bullet-}$ and electrophilic P_k^+ Parr function of **TCAN2**.

about the electron density shared between neighboring atoms can be extracted [57].

A great deal of work has confirmed that the ELF topological analysis of the bonding changes along a reaction path is a powerful tool to establish the molecular mechanism of a reaction [59,60,57]. After an analysis of the electron density, ELF provides basins that are the domains in which the probability of finding an electron pair is maximal. The basins are classified as core and valence basins. The latter are characterized by the synaptic order, *i.e.* the number of atomic valence shells in which they participate [61]. Thus, there are monosynaptic, disynaptic, trisynaptic basins, and so on. Monosynaptic basins, labelled as V(A), correspond to lone pairs or non-bonding regions, while disynaptic basins, labelled as V(A,B), connect the core of two nuclei A and B and, thus, correspond to a bonding region between A and B. This description recovers the Lewis bonding model, providing a very suggestive graphical representation of the molecular system.

The ELF topological analysis of significant organic reactions involving the formation of new C–C single bonds has shown that it begins in the short C–C distance range of 1.9–2.0 Å by merging two monosynaptic basins, V(Cx) and V(Cy), into a new disynaptic basin V(Cx,Cy) associated with the formation of the new Cx–Cy single bond [39]. The Cx and Cy carbons characterized by the presence of the monosynaptic basins, V(Cx) and V(Cy), are called *pseudo-radical* centers [62].

In order to understand the molecular mechanism of the 32CA reaction between **BNS1** and **TCAN2**, an ELF topological analysis of the MPWB1 K/6-311G(d) wave functions of some relevant points, **P1** through **P5**, was performed along the IRC profile associated with the more favorable **TS1**. The details of the ELF topological analysis are given in the electronic supplementary information.

Considering ELF patterns and their changes along the considered points **P1** through **P5** located on the IRC curve of more favorable **TS1** (Fig. S1, Supplementary data), some appealing points can be summarized as follows:

- both S3–C4 and C1–N5 single-bond formations take place after passing TS1;
- the formation of C1–N5 single bonds at **P4**, d(C1–N5) = 1.813 Å occurs prior to the formation of the S3–C4 single bonds at **P5**, d(S3–C4) = 2.008 Å. On the other hand, S3–C4 single-bond formation is accompanied with the completion of C1–N5 single-bond formation by more than of 83%, portraying a very asynchronous process via a *two-stage one-step* molecular mechanism;
- while C1–N5 single-bond formation takes place via the nucleophilic attack of a C1 carbon atom on the highly electrophilic N5 nitrogen atom in which N5, unlike C1, does not participate as a *pseudoradical* center, the formation of a S3–C4 single bond presents a completely different pattern following Domingo's model [63,53]. In other words, S3–C4 single-bond formation takes place by the creation of two S3 and C4 *pseudoradical* centers characterized by the presence of V″(S3) and V(C4) monosynaptic basins, followed by their merging into a V(S3,C4) disynaptic basin;
- according to the patterns involved in the formation of S3–C4 and C1–N5 single bonds, the pericyclic mechanism for cycloaddition reactions in which a concerted movement is suggested for electrons [64] should be rejected.

4. Conclusion

The [3+2] cycloaddition (32CA) reaction of benzonitrile sulfide **BNS1** toward trichloroacetonitrile **TCAN2** in the presence of toluene, experimentally studied by Greig et al., was theoretically investigated at the MPWB1 K/6-311G(d) level. In clear agreement with experimental outcomes, the energetic studies of reaction paths involved in the 32CA reaction between **BNS1** and **TCAN2** obviously showed that this reaction in the gas phase as well as in the presence of toluene carried out via the extremely regioselective (regiospecific) C1–N5 channel furnishes the aromatic five-membered heterocyclic cycloadduct **CA1**, 3-phenyl-5-(trichloromethyl)-1,2,4-thiadiazole, as the unique kinetically and thermodynamically observable yield.

Analysis of the global DFT reactivity indices indicates that the strong nucleophilic character of **BNS1** and the strong electrophilic character of **TCAN2**, caused by the presence of a highly electron-withdrawing CCl_3 substitution, are responsible for a high polar character in the studied 32CA reaction, presenting a noticeable GEDT value of 0.27e in the more favorable **TS1**.

Calculated electrophilic and nucleophilic Parr functions at the interacting sites of reagents indicate that while the most electrophilic center in **TCAN2** is N5 nitrogen atom, possessing the maximum electrophilic P_k^- Parr function of 0.26, the most nucleophilic center in **BNS1** is S3 sulfur atom, possessing the maximum nucleophilic P_k^+ Parr function of 0.89. Consequently, it is predicted that the most nucleophilic S3 center in **BNS1** is attacked by the most electrophilic N5 one in **TCAN2**, initializing the corresponding 32CA reaction via **TS2**. Amusingly, such prediction is completely against the energetic results. Indeed, the steric repulsion interaction between large chlorine substitutions and the phenyl ring, on the one hand, and the steric hindrance between lone pairs of S3 sulfur and N5 nitrogen atoms, on the other one, account for the lack of predominance **TS2**. Therefore, it evidences that, in the case under study, steric repulsion effects play a more important role than the electronic ones and, thus, control the total regioselectivity observed experimentally.

The ELF analysis performed on the considered 32CA reaction clarifies interesting points about the molecular mechanism of this reaction in which carbon–heteroatoms interactions lead to generating the corresponding cycloadduct. In this relation, while the S3–C4 single-bond formation at a distance of 2.008 Å takes place exactly according to the model proposed by Domingo [63,53], the formation of a C1–N5 single bond, prior to that of the S3–C4 one, at a shorter distance of 1.813 Å, follows a quite different pattern. In other words, the depopulation of C4–N5 and N2–S3 bonds followed by the formation of two non-bonding V(C4) and V″(S3) monosynaptic basins and, then, by the merging of two aforementioned monosynaptic basins into one V(S3,C4) disynaptic basin, portrays the mechanism of

S3–C4 single-bond formation. On the other hand, the C1–N5 single-bond formation occurs through the nucleophilic attack of the C4 carbon atom on the electrophilic N5 nitrogen atom. The patterns obtained via ELF topological analysis authoritatively allow us to reject the pericyclic mechanism for cycloaddition reactions in which a concerted movement is suggested for electrons [64].

Appendix A. Supplementary data

Supplementary data associated with this article can be found, in the online version, at http://dx.doi.org/10.1016/j.crci.2015.09.003.

References

[1] W. Carruthers, Cycloaddition reactions in organic synthesis, Pergamon, Oxford, 1990.
[2] S.R. Emamian, E. Zahedi, J. Phys. Org. Chem. 25 (2012) 748.
[3] S.R. Emamian, S. Ali-Asgari, E. Zahedi, J. Chem. Sci. 126 (2014) 293.
[4] S.R. Emamian, T. Lu, F. Moeinpour, RSC Adv. 5 (2015) 62248.
[5] L.R. Domingo, M.J. Aurell, P. Pérez, Tetrahedron 70 (2014) 4519.
[6] L.R. Domingo, S.R. Emamian, Tetrahedron 70 (2014) 1267.
[7] B. Braida, C. Walter, B. Engels, P.C. Hiberty, J. Am. Chem. Soc. 132 (2010) 7631.
[8] D.J. Greig, D.G. Hamilton, M. McPherson, R.M. Paton, J. Chem. Soc., Perkin Trans. 1 (1987) 607.
[9] R.S. Kumar, S.M. Rajesh, S. Perumal, P. Yogeeswari, D. Sriram, Tetrahedron: Asymmetry 21 (2010) 1315.
[10] S. Chen, J. Ren, Z. Wang, Tetrahedron 65 (2009) 9146.
[11] V.M. de Almeida, R.J. dos Santos, A.J. da Silva Góes, J.G. de Lima, C.R. Duarte Correia, A.R. de Faria, Tetrahedron Lett. 50 (2009) 684.
[12] P. Bujak, S. Krompiec, J. Malarz, M. Krompiec, M. Filapek, W. Danikiewicz, M. Kania, K. Gębarowska, I. Grudzka, Tetrahedron 66 (2010) 5972.
[13] C.L. Yoo, M.M. Olmstead, D.J. Tantillo, M.J. Kurth, Tetrahedron Lett. 47 (2006) 477.
[14] K. Hemming, A.B.N. Luheshi, A.D. Redhouse, R.K. Smalley, J.R. Thompson, P.D. Kennewell, R. Westwood, Tetrahedron 49 (1993) 4383.
[15] E. Coutouli-Argyropoulou, E. Thessalonikeos, J. Heterocycl. Chem. 28 (1991) 429.
[16] G. Wang, X. Liu, T. Huang, Y. Kuang, L. Lin, X. Feng, Org. Lett. 15 (2013) 76.
[17] A.J. Morrison, R.M. Paton, R.D. Sharp, Synth. Commun. 35 (2005) 807.
[18] J.E. Franz, L.L. Black, Tetrahedron Lett. 11 (1970) 1381.
[19] R.M. Paton, Chem. Soc. Rev. 18 (1989) 33.
[20] M.J. Sanders, J.R. Grunwell, J. Org. Chem. 45 (1980) 3753.
[21] R.K. Howe, T.A. Gruner, L.G. Carter, L.L. Black, J.E. Franz, J. Org. Chem. 43 (1978) 3736.
[22] R.K. Howe, J.E. Franz, J. Org. Chem. 39 (1974) 962.
[23] A.M. Damas, R.O. Gould, M.M. Harding, R.M. Paton, J.F. Ross, J. Chem. Soc., Perkin Trans. 1 (1981) 2991.
[24] K.F. Wai, M.P. Sammes, J. Chem. Soc., Perkin Trans. 1 (1991) 183.
[25] R.K. Howe, T.A. Gruner, J.E. Franz, Org. Chem. 42 (1977) 1813.
[26] M.C. McKie, R.M. Paton, Arkivoc vi 15 (2002).
[27] P.A. Datar, T.A. Deokule, Med. Chem. 4 (2014) 390.
[28] V. Palomo, D.I. Perez, C. Perez, J.A. Morales-Garcia, I. Soteras, S. Alonso-Gil, A. Encinas, A. Castro, N.E. Campillo, A. Perez-Castillo, C. Gil, A. Martinez, J. Med. Chem. 55 (2012) 1645.
[29] B. Sharma, A. Verma, S. Prajapati, U.K. Sharma, Int. J. Med. Chem. 2013 (2013) 1.
[30] S. Jalhan, A. Jindal, A. Gupta, Hemraj, Asian J. Pharm. Clin. Res. 5 (2012) 199.
[31] M. Asif, Am. J. Curr. Org. Chem. 1 (2014) 17.
[32] K.A. Kumar, G.V. Kumar, N. Renuka, Int. J. PharmTech. Res. 5 (2013) 239.
[33] D.J. Greig, M. McPherson, R.M. Paton, J. Crosby, Phosphorus, Sulfur Silicon Relat. Elem. 26 (1986) 151.
[34] A. Savin, A.D. Becke, J. Flad, R. Nesper, H. Preuss, H.G. Von Schnering, Angew. Chem. Int. Ed. 30 (1991) 409.
[35] B. Silvi, A. Savin, Nature 371 (1994) 683.
[36] A. Savin, B. Silvi, F. Colonna, Can. J. Chem. 74 (1996) 1088.
[37] A. Savin, R. Nesper, S. Wengert, T.F. Fassler, Angew. Chem. Int. Ed. Engl. 36 (1997) 1808.
[38] K. Fukui, J. Phys. Chem. 74 (1970) 4161.
[39] Y. Zhao, D.G. Truhlar, J. Phys. Chem. A 108 (2004) 6908.
[40] W.J. Hehre, L. Radom, P.V.R. Schleyer, J.A. Pople, Ab initio Molecular Orbital Theory, Wiley, New York, 1986.
[41] X. Li, M.J. Frisch, J. Chem. Theory Comput. 2 (2006) 835.
[42] H.P. Hratchian, H.B. Schlegel, J. Chem. Phys. 120 (2004) 9918.
[43] J. Tomasi, M. Persico, Chem. Rev. 94 (1994) 2027.
[44] V. Barone, M. Cossi, J. Tomasi, J. Comput. Chem. 19 (1998) 404.
[45] A.E. Reed, R.B. Weinstock, F. Weinhold, J. Chem. Phys. 83 (1985) 735.
[46] S. Noury, X. Krokidis, F. Fuster, B. Silvi, Comput. Chem. 23 (1999) 597.
[47] M.J. Frisch, G.W. Trucks, H.B. Schlegel, G.E. Scuseria, M.A. Robb, J.R. Cheeseman, G. Scalmani, V. Barone, B. Mennucci, G.A. Petersson, H. Nakatsuji, M. Caricato, X. Li, H.P. Hratchian, A.F. Izmaylov, J. Bloino, G. Zheng, J.L. Sonnenberg, M. Hada, M. Ehara, K. Toyota, R. Fukuda, J. Hasegawa, M. Ishida, T. Nakajima, Y. Honda, O. Kitao, H. Nakai, T. Vreven, J.A. Montgomery Jr., J.E. Peralta, F. Ogliaro, M. Bearpark, J.J. Heyd, E. Brothers, K.N. Kudin, V.N. Staroverov, R. Kobayashi, J. Normand, K. Raghavachari, A. Rendell, J.C. Burant, S.S. Iyengar, J. Tomasi, M. Cossi, N. Rega, J.M. Millam, M. Klene, J.E. Knox, J.B. Cross, V. Bakken, C. Adamo, J. Jaramillo, R. Gomperts, R.E. Stratmann, O. Yazyev, A.J. Austin, R. Cammi, C. Pomelli, J.W. Ochterski, R.L. Martin, K. Morokuma, V.G. Zakrzewski, G.A. Voth, P. Salvador, J.J. Dannenberg, S. Dapprich, A.D. Daniels, O. Farkas, J.B. Foresman, J.V. Ortiz, J. Cioslowski, D.J. Fox., Gaussian 09, (Revision A.02-SMP), Gaussian Inc, Wallingford, CT, 2009
[48] R.G. Parr, L. Von Szentpaly, S.B. Liu, J. Am. Chem. Soc 121 (1999) 1922.
[49] R.G. Parr, W. Yang, Density Functional Theory of atoms and molecules, Oxford University Press, New York, 1989.
[50] L.R. Domingo, E. Chamorro, P. Pérez, J. Org. Chem. 73 (2008) 4615.
[51] W. Kohn, L. Sham, Phys. Rev. 140 (1965) 1133.
[52] L.R. Domingo, P. Pérez, J.A. Sáez, RSC Adv. 3 (2013) 1486.
[53] L.R. Domingo, RSC Adv. 4 (2014) 32415.
[54] P. Geerlings, F. De Proft, W. Langenaeker, Chem. Rev. 103 (2003) 1793.
[55] L.R. Domingo, M.J. Aurell, P. Pérez, R. Contreras, Tetrahedron 58 (2002) 4417.
[56] P. Jarmillo, L.R. Domingo, E. Chamorro, P. Pérez, J. Mol. Struct. (THEOCHEM) 865 (2008) 68.
[57] J. Andrés, S. Berski, L.R. Domingo, P. González-Navarrete, J. Comput. Chem. 33 (2012) 748.
[58] A.D. Becke, K.E. Edgecombe, J. Chem. Phys. 92 (1990) 5397.
[59] V. Polo, J. Andrés, S. Berski, L.R. Domingo, B. Silvi, J. Phys. Chem. A 112 (2008) 7128.
[60] J. Andrés, S. Berski, L.R. Domingo, V. Polo, B. Silvi, Curr. Org. Chem. 15 (2011) 3566.
[61] B. Silvi, J. Mol. Struct. 614 (2002) 3.
[62] L.R. Domingo, E. Chamorro, P. Pérez, Lett. Org. Chem. 7 (2010) 432.
[63] M. Ríos-Gutiérrez, P. Pérez, L.R. Domingo, RSC Adv. 5 (2015) 58464.
[64] F.A. Carey, R.J. Sundberg, Advanced organic chemistry. Part A: structure and mechanisms, Springer, New York, 2000